



## Article

# Improving Energy Efficiency and Autonomy Through the Development of a Hybrid Battery–Supercapacitor System in Electromobility

Michalakis Kotsias, Georgios Kontogogos, Spyridon Angelopoulos  and Evangelos Hristoforou \* 

School of Electrical and Computer Engineering, National Technical University of Athens, GR-15772 Athens, Greece; mihaliskoca@hotmail.com (M.K.); spyrosag@central.ntua.gr (S.A.)

\* Correspondence: hristoforou@ece.ntua.gr; Tel.: +30-2107722178

**Abstract:** This study focuses on the development of a hybrid battery-supercapacitor system aimed at enhancing energy efficiency and autonomy in electromobility. The energy supply system of an electric vehicle must ensure high performance and autonomy, even after numerous battery life cycles. Previous approaches to hybrid systems that combine batteries and supercapacitors focus on reducing power losses by relying on controllers that evaluate the state of charge (SOC) of the energy sources to determine which one should provide power at any given time. These systems typically use a controller that monitors only the SOC of the battery and supercapacitor. In contrast, our study introduces an innovative controller that not only evaluates the SOC of both energy sources but also incorporates the current of the electric motor, taking into account its operational state. This approach allows for a more accurate representation of energy consumption and motor performance, providing significant advantages in terms of energy efficiency, extended battery life, and improved performance under high motor loads, which are characteristic of modern electric vehicle requirements. The current paper encompasses both experimental and simulated results, indicating that the hybrid approach provides significant advantages, such as improved energy autonomy, extended battery life as the primary energy source, and enhanced performance at high motor speeds that stress the battery.



Academic Editor: Tek Tjing Lie

Received: 14 November 2024

Revised: 21 December 2024

Accepted: 25 December 2024

Published: 28 December 2024

**Citation:** Kotsias, M.; Kontogogos, G.; Angelopoulos, S.; Hristoforou, E. Improving Energy Efficiency and Autonomy Through the Development of a Hybrid Battery–Supercapacitor System in Electromobility. *Energies* **2025**, *18*, 76. <https://doi.org/10.3390/en18010076>

**Copyright:** © 2024 by the authors. Licensee MDPI, Basel, Switzerland. This article is an open access article distributed under the terms and conditions of the Creative Commons Attribution (CC BY) license (<https://creativecommons.org/licenses/by/4.0/>).

**Keywords:** hybrid energy system; battery aging; supercapacitor; controller

## 1. Introduction

One of the most critical systems of an electric vehicle is the power supply for the electric motor, with batteries being the primary source. The performance of an electric vehicle largely depends on the efficiency of its batteries, making their operation vital. A significant issue affecting battery efficiency is the reduction of capacity over time. Battery aging has attracted the attention of automotive manufacturers and researchers, as understanding and identifying the causes of this process is essential for developing improvement strategies [1].

The main causes of battery aging include the number of life cycles, temperature, state of charge (SOC) level, load type, charging rate, and usage conditions [1]. Each time the battery is charged and discharged, it experiences minor wear, and extreme temperatures can accelerate this aging process. To address battery aging, various methods have been implemented in modern automotive engineering, including the use of supercapacitors as a secondary power source. These innovations aim to enhance battery performance and longevity, ensuring more efficient energy management in electric vehicles.

In conclusion, the causes of battery aging are numerous and vary in significance. The following sections will focus on life cycles, SOC levels, and the load current demand [1]. One promising method for reducing battery fatigue is the introduction of supercapacitors as a secondary power source. Supercapacitors, or electrostatic capacitors, are energy devices that store electrical energy through electrostatic fields, offering numerous advantages over traditional batteries. They have a high-power density, allowing for rapid energy supply to the motor during peak demand periods, such as starting and acceleration [2,3]. Furthermore, supercapacitors exhibit excellent resistance to temperature variations and can operate effectively across a wide range of temperatures.

Supercapacitors offer significant advantages, such as high-power density and the ability to charge and discharge quickly. This technology is ideal for situations with increased power demands, like vehicle starting and acceleration. However, despite their development, batteries remain a crucial energy source, offering high energy density, which is essential for long-term energy storage and the autonomy of electric vehicles [4].

The purpose of this article is to analyze the collaboration between batteries and supercapacitors in a hybrid energy system, focusing on improving energy efficiency and autonomy in electric mobility through the simulation of a controller that manages both energy sources. The controller will consider parameters, such as battery cycles, SOC levels, and load current, to ensure appropriate energy distribution and maximize the power supply system's performance.

## 2. Simulation of Power Sources

The simulation of the elements of the hybrid energy storage system we have developed through Matlab/Simulink 10.7 will focus on the collaboration of two main sources: batteries and supercapacitors [5]. This approach allows for a comprehensive analysis of their behavior and electrical characteristics, as well as the evaluation of their interaction under various load conditions. In Simulink, 10.7 the simulation of batteries includes the modeling of critical parameters such as capacity, discharge voltage, and internal resistance. These simulations facilitate the analysis of battery performance under different scenarios, including charging and discharging. The ability to simulate battery aging provides valuable insights into the prediction of capacity degradation over time.

The simulation of supercapacitors in Simulink requires detailed modeling. The platform enables the creation of models that examine the unique response of supercapacitors to high currents and transient states.

The combined analysis of batteries and supercapacitors through Simulink will allow us to create the hybrid energy storage system we have designed, offering advantages such as improved performance and increased system operation.

### 2.1. Battery Model Overview

The battery model contains a battery, a controlled current source, and a battery cycle generator. The parameters used for the battery model refer to each cell individually, not the pack of three batteries that outputs 12 volts, as described in the experimental measurements (Figure 1). The battery is designed with a nominal voltage of 3.7 volts, which provides a stable power output during operation. When fully charged, the voltage reaches 4 volts, allowing for optimal performance. Its capacity is rated at 2900 mAh, enabling it to store a significant amount of energy for extended use. Additionally, the cut-off voltage is set at 2.775 volts, ensuring that the battery is protected from deep discharging.

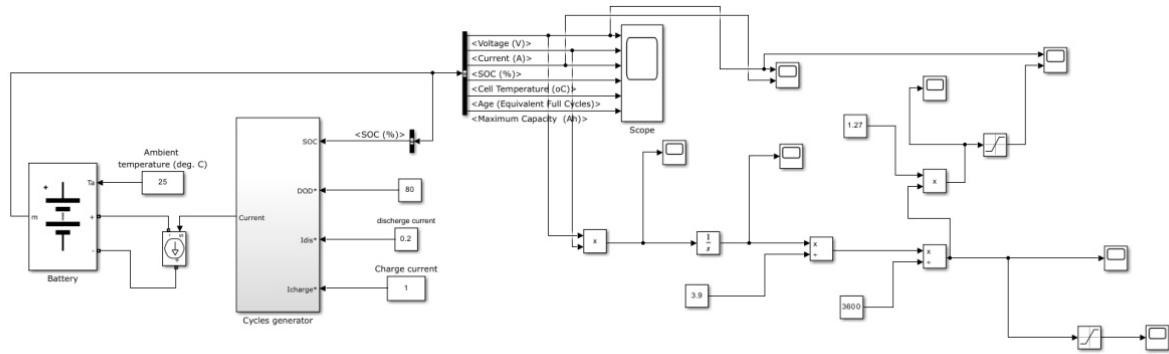


**Figure 1.** The Li-ion Battery Model in Simulink.

### 2.1.1. Charging and Discharging Behavior of Battery

The cycle generator model processes the charging and discharging currents of the battery, effectively determining whether the battery is in a charging or discharging state [6]. Experimental measurements indicated that the motor consumes a current of 0.2 A, while its nominal load is 1.2 A. The simulation explored a range of currents from 0.2 A to 1.2 A, as illustrated in Figure 2.

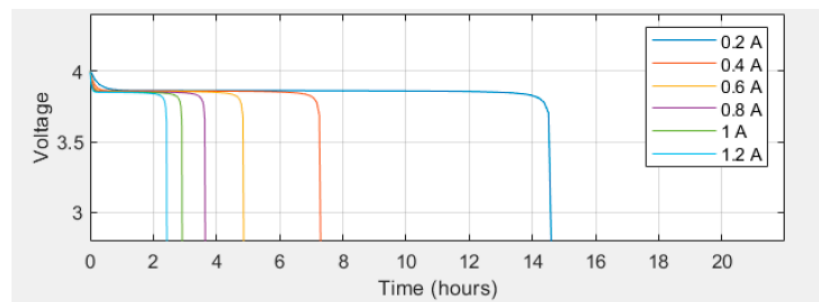


**Figure 2.** Battery behavior for various load current (0.2–1.2 A).

The battery completely discharges in approximately 14.5 h, exhibiting a voltage decline during the first 14 h, followed by a sharp drop in the final 30 min. When simulating higher currents, the battery voltage decreases more rapidly, as anticipated. Additionally, simulations examined the relationship between battery voltage and capacity in ampere-hours (Ah), revealing minimal differences in current (Figure 3). This similarity resulted in nearly indistinguishable voltage-capacity curves.

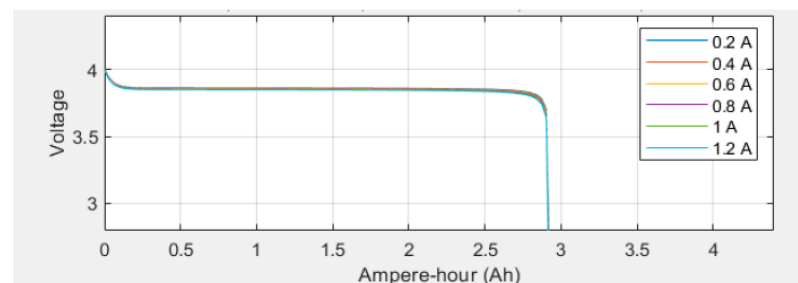


**Figure 3.** Voltage and capacity of battery for various load currents.

### 2.1.2. Cycle and Battery Capacity Decreases

Further simulations were conducted to evaluate the battery's performance after multiple cycles [6]. In these simulations, the charging current was fixed at 1 A, while the discharging current remained at 0.2 A, replicating the laboratory procedures. The full

charging process typically takes around 2.5 to 3 h, whereas full discharging requires about 14.5 h. Consequently, each complete charge–discharge cycle lasts approximately 17 h.

After 36 cycles, the capacity reduces to about 2.4 Ah, reflecting a decline of approximately 0.5 Ah. After 72 cycles, this capacity further decreases to around 1.9 Ah. By the time the battery has completed 144 cycles, its capacity falls below 1 Ah, rendering it inadequate for our intended application (Figure 4).

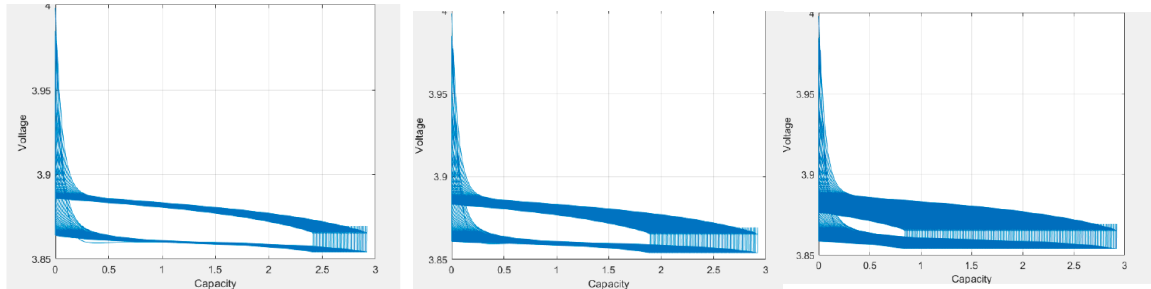


**Figure 4.** Behavior of battery cell capacity and voltage for 36 (left), 72 (middle), and 144 (right) cycles.

After reaching a specific number of cycles (135 cycles), and when the capacity drops below 1 Ah, supercapacitors should be employed to assist in delivering power during normal operational conditions as well.

## 2.2. Supercapacitor Simulation

The supercapacitor model was created in LT-Spice, and two simulations were conducted. The first simulation corresponds to charging the supercapacitor with a constant voltage of 5 volts and a constant current of 0.1 A [7–9]. The second simulation pertains to discharging it with a current of 0.33 A, as shown in Figure 5. This discharge current was chosen based on experimental measurements where the current started from 0.4 A and decreased to 0.25 A, resulting in an average current of approximately 0.33 A.

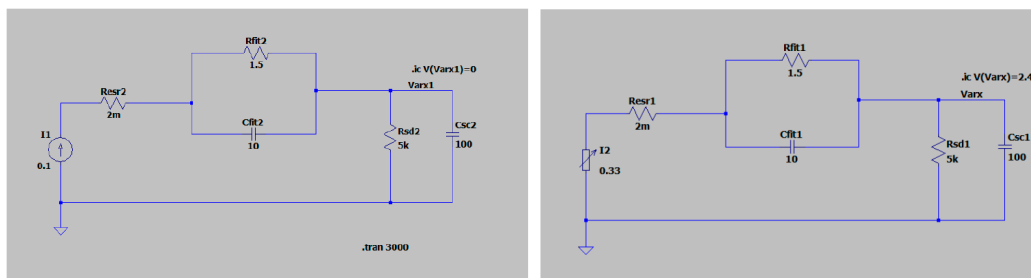


**Figure 5.** The supercapacitor LT spice model for the charging (left circuit) and discharging process (right circuit).

The supercapacitor used in this study has a capacitance ( $C_{sc}$ ) of 100 Farads and a self-discharge resistance ( $R_{sd}$ ) of 5 k $\Omega$ . The equivalent series resistance ( $E_{SR}$ ) is 2 m $\Omega$ . Initially, the supercapacitor was fully discharged, and its starting voltage during charging was 0 volts. During discharge, the initial voltage was about 2.4 volts when the discharge started.

### 2.2.1. Simulation Results

The time required to fully charge the supercapacitor to 2.7 volts at a constant current of 0.1 A is 2700 s, or 45 min, as shown in Figure 6.

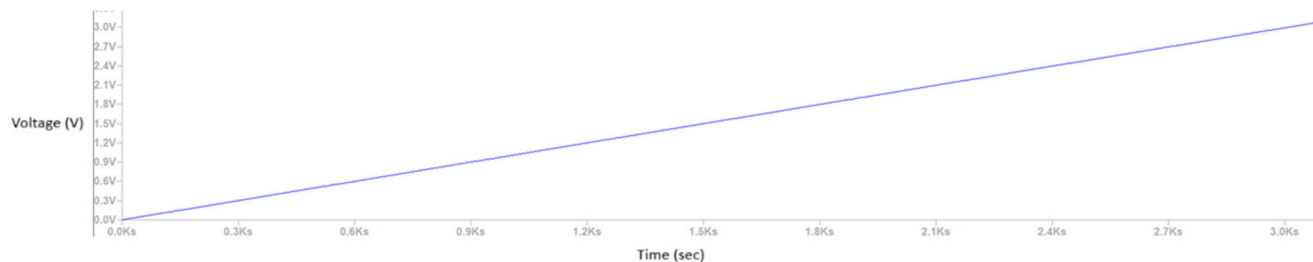


**Figure 6.** Supercapacitor charging time.

On the other hand, the time required for total discharge from 2.4 volts is 730 s, or 12 min (Figure 7). It is evident that discharging occurs much more rapidly than charging.

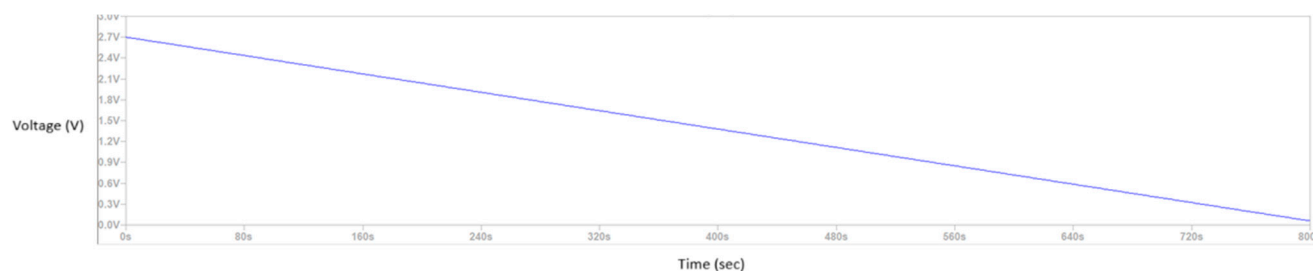


**Figure 7.** Supercapacitor discharging time.

### 2.2.2. Load Current and Supercapacitor Discharge Time

To examine the behavior of the supercapacitor under various load current values, tests were performed in LT-Spice across a range of currents from 0.05 A to 1.5 A, with a step of 0.05 A. For a load current of 0.05 A, the discharge time is 89.5 min. As the current increases to 0.5 A, the discharge time significantly decreases to 9 min. Further increasing the current to 1.5 A reduces the discharge time to 2.9 min. Figure 8 represents the dependence of current on the discharging current.

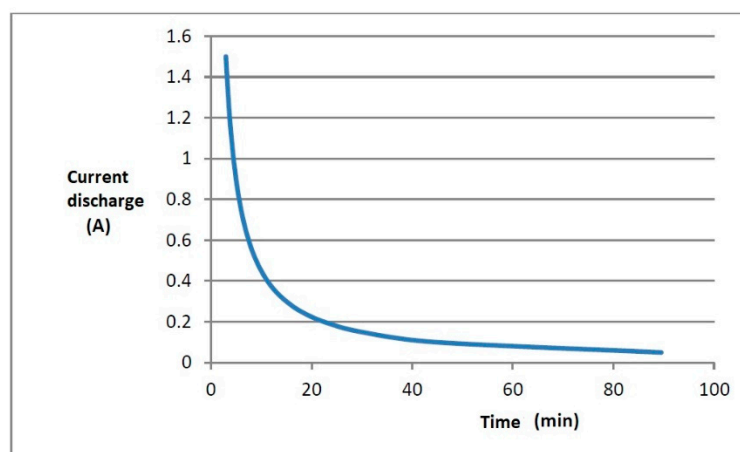


**Figure 8.** Supercapacitor discharge time for values load current up to 1.5 A.

These tests are important because supercapacitors are used in hybrid systems to power electric motors during start-up and acceleration, times when the demand for current is high.

## 3. Experimental Analysis of Battery and Supercapacitor Performance

### 3.1. Experimental Analysis of Batteries as Main DC Motor Power Sources

For the experimental measurements, three Li-ion batteries with a capacity of 2900 mAh and a nominal voltage of 3.7 volts were utilized. These batteries were connected in series

to power a 12 volt, 1.2 A DC motor. A PWM microcontroller was installed between the batteries, allowing the motor speed to be controlled. The microcontroller has a switch that makes it easy to adjust the motor speed from 10% to 100% of maximum speed. The experimental setup is illustrated in Figure 9.

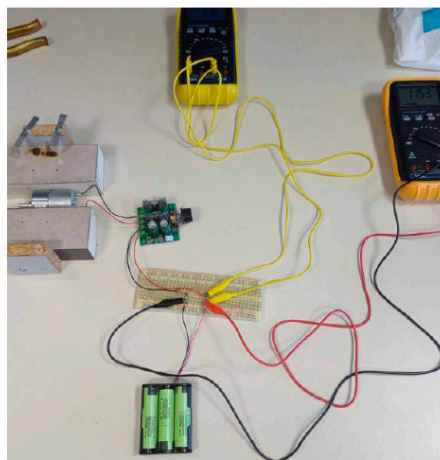


**Figure 9.** Experimental setup of batteries pack, PWM controller, and DC motor.

Prior to commencing the steady-state measurements, three starting tests were conducted to capture the maximum starting current of the motor. The recorded values were as follows: during the first start, the voltage was 12.01 volts with a maximum current of 0.3 A; during the second start, the voltage reached 12.02 volts with a maximum current of 0.27 A; and during the third start, the voltage increased to 12.04 volts with a maximum current of 0.43 A.

After approximately 25 h of measurements in steady-state operation at maximum speeds, the results for the current and voltage of the batteries revealed that the voltage across the battery pack initially started at 12 volts and gradually decreased until around 24 h, where a sharp decline in performance was observed (Figure 10). Correspondingly, the current supplied to the motor decreased as the voltage dropped.

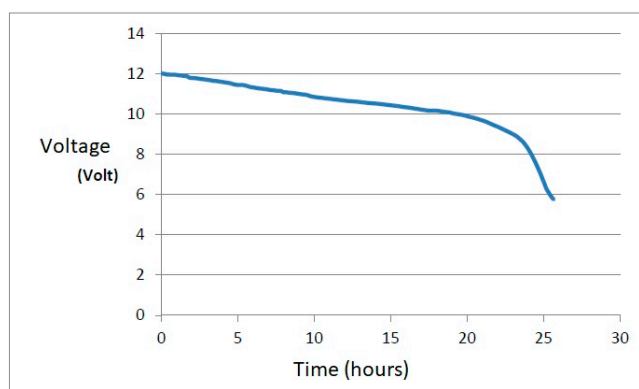


**Figure 10.** Voltage of the battery pack.

When the voltage across the pack fell below 7 volts, the motor's rotor began to spin at a noticeably lower speed. When the voltage dropped below 6 volts, the rotor struggled to turn, and at a voltage of 5.75 volts, the motor completely stopped. At the conclusion of the experiment, the final voltage at the terminals of each battery was measured. The final voltage for the first battery was 2.27 volts, for the second battery it was 1.678 volts, and for the third battery it was 2.939 volts.

### 3.1.1. Battery Voltage and Capacity Relationship

The Li-ion battery has a nominal voltage of approximately 3.6 V to 3.7 V, reaching up to 4.2 V when fully charged. As the battery discharges, the voltage drops below 3 V. During experiments with a constant load current of 0.2 A, it was observed that the motor stopped functioning after 25.67 h, while the voltage dropped below 3 V after 23 h (Figure 11). When the total voltage of the three-battery pack reached 9 V, it was concluded that each battery had dropped to 3 V at that point, resulting in a calculated capacity of 4600 mAh. Laboratory measurements confirmed that the discharge time was around 23 h, with the capacity remaining above 4000 mAh, exhibiting slight fluctuations due to variations in current (ranging from 0.17 A to 0.2 A). A simulation in LT-Spice and Simulink, with a load current of 0.2 A and a capacity of 4600 mAh, yielded expected results (Figure 12). Figure 13 represents experimental results that align with the Simulink results.

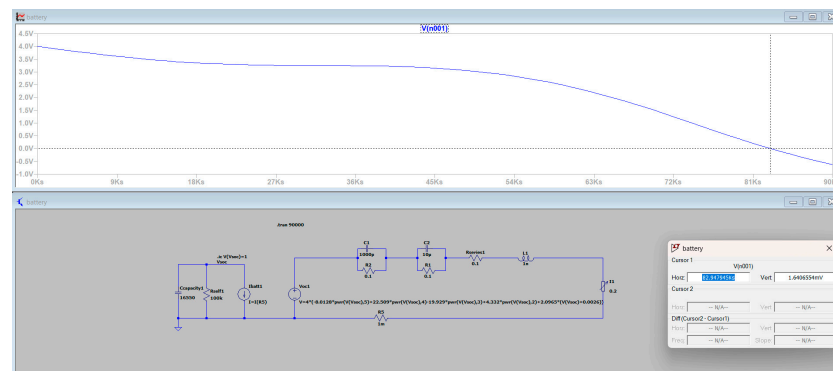


Figure 11. Voltage of the battery pack. in LT-Spice simulation.

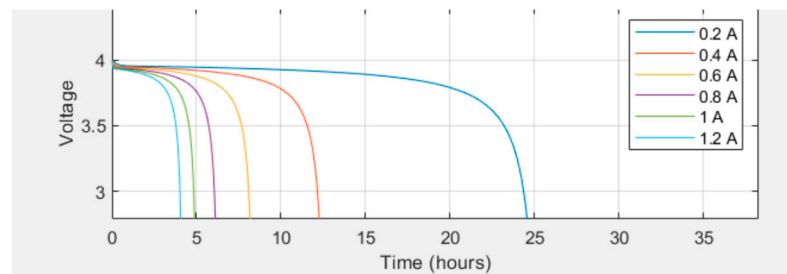


Figure 12. The voltage of the battery for a simulation with load currents from 0.2 A to 1.2 A and a capacity of 4600 mAh on Simulink.

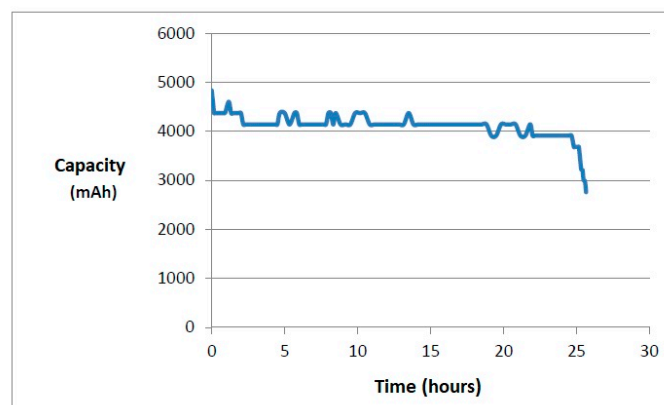


Figure 13. The capacity of the batteries during the laboratory measurements.

### 3.1.2. Battery State of Capacity (SOC)

The correlation between the battery voltage and its state of charge (SOC) will be established using the integral method [10,11]. The SOC is calculated using the following formula:

$$\text{SOC}(\%) = \frac{Q}{Q_{\max}} \times 100, \quad (1)$$

where  $Q$  is the estimated charged energy quantity and  $Q_{\max}$  is the maximum possible charged energy quantity. To calculate  $Q$ , the following equation is used:

$$Q = \int_{t_0}^t (I_{\text{in}} - I_{\text{on}}) dt. \quad (2)$$

In our case,  $I_{\text{in}}$  is zero. Therefore, the negative sign does not affect the calculation, as the absolute value will be taken. Thus,  $Q$  is computed as

$$Q = I_{\text{out}} \times (t - t_0). \quad (3)$$

This procedure was applied to the measurements obtained from the laboratory, where each measured current value was multiplied by the time interval of 10 min and subsequently converted to Coulombs. For the calculation of  $Q_{\max}$ , the first measurement, where the current was 0.21 A (i.e., at its maximum), was considered. Thus, we have

$$Q_{\max} = 2.1 \text{ A} \times \text{min} = 126. \quad (4)$$

Finally, by applying the relationship (1), it is observed that the SOC follows the behavior of the battery current, experiencing a sharp decline at 23 h, when the battery voltage drops to 3 volts (Figure 14).

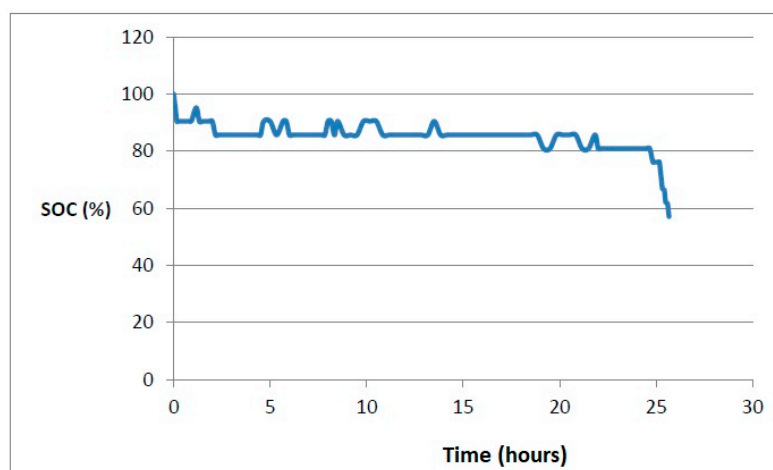


**Figure 14.** The SOC of the batteries during laboratory measurements.

### 3.2. Experimental Analysis of Supercapacitor as Main DC Motor Power Source

For the laboratory measurements, 100 Farad supercapacitors were utilized. These supercapacitors are known for their ability to store and discharge energy rapidly, making them ideal for applications that require quick bursts of power. Their high capacitance allows for significant energy storage, which is essential in experiments involving energy transfer and efficiency assessment.



### 3.2.1. Parameters of Supercapacitor Charging

The two supercapacitors were connected to the generator, which was set to supply a current of 0.1 A with a constant DC voltage of 5 volts [9,12]. The measurement results for the charging of the two supercapacitors are shown in Figure 15. The initial voltages of the supercapacitors before charging were 0.455 V and 0.502 V. As shown by the resulting curves, each supercapacitor took approximately 40 min to reach a terminal voltage of 2.5 V.

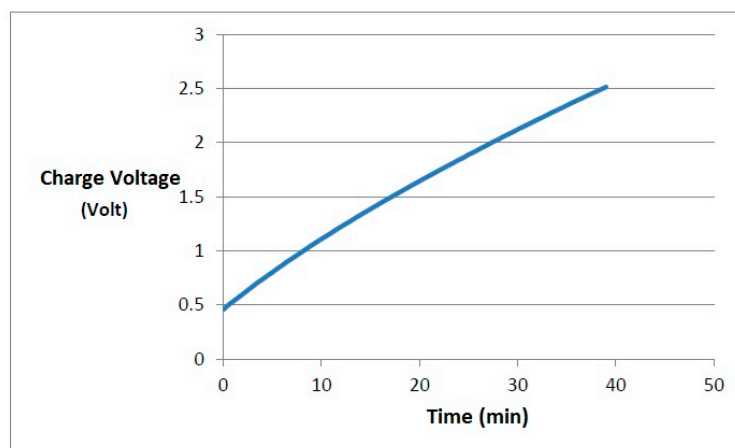


Figure 15. The charging voltage of supercapacitor of 100 Farads versus time.

In the LT-Spice simulation, the time required for the supercapacitor to fully charge was 45 min, starting from 0 V. The laboratory measurements are very close to the simulation results, both in charging time and in the shape of the curve, as the increase in voltage was exactly as expected, that is, nearly linear.

### 3.2.2. Parameters of Supercapacitor Discharging

For discharging, a smaller motor was used compared to the one used for discharging the batteries, because the previous 12 V motor could not start due to the low voltage provided by the supercapacitors, which have a maximum voltage of 2.8 V. Therefore, we used a 1.5 V motor. The supercapacitors were connected directly to the motor without a PWM microcontroller, resulting in the motor running at maximum speed depending on the voltage, which initially was 2.4 V and decreased as the supercapacitor discharged (Figures 16 and 17 show voltage and current dependence based on time, respectively).

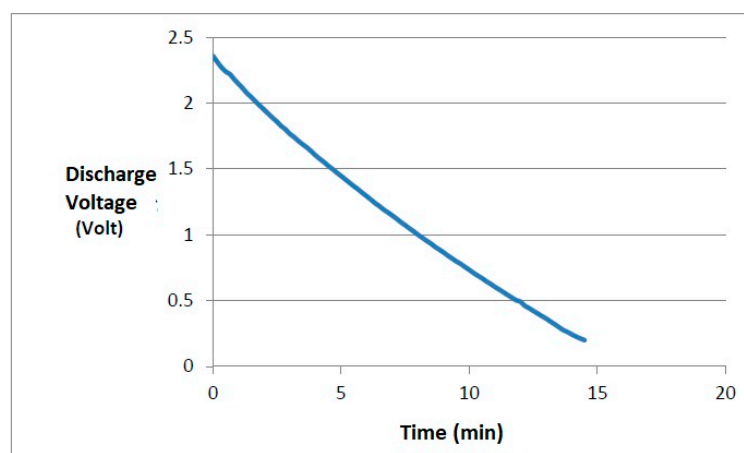
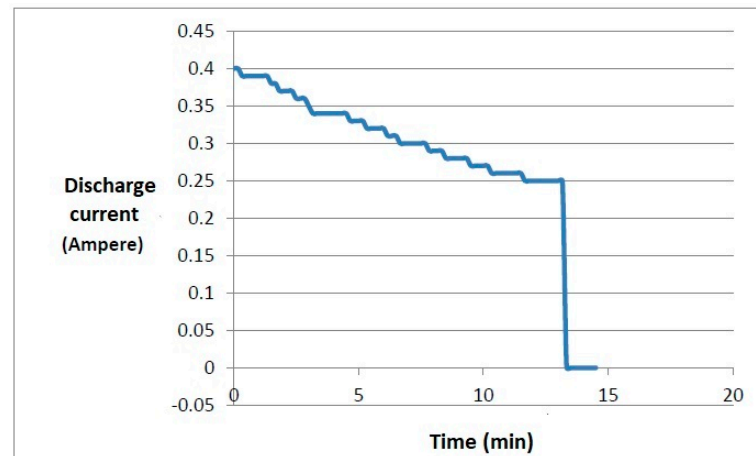


Figure 16. Discharge voltage of the 100 Farad supercapacitor versus time.



**Figure 17.** Discharge current of the 100 Farad supercapacitor.

For discharging, a smaller motor was used compared to the one used for discharging the batteries, as the previous 12 V motor could not start due to the low voltage provided by the supercapacitors, which have a maximum voltage of 2.8 V. Therefore, a 1.5 V motor was used. The supercapacitors were connected directly to the motor without a PWM microcontroller, causing the motor to run at maximum speed depending on the voltage, which initially was 2.4 V and decreased as the supercapacitors discharged (Figures 16 and 17 show the voltage and current dependence based on time, respectively).

The measurement results for each supercapacitor show that the first supercapacitor discharged in nearly 15 min, while the simulation indicated 12 min. This small difference may be due to the current not being constant at 0.33 A but rather starting at 0.4 A and then decreasing to 0.25 A. The sharp drop in current around 14 min indicates the stalling of the motor, as the voltage from the supercapacitor dropped below 0.5 V, which is insufficient to drive the rotor [9].

#### 4. Hybrid Power Supply System

The importance of the energy supply system in an electric vehicle lies in achieving high autonomy and efficiency, especially as batteries wear out. A hybrid system that combines the strengths of batteries and supercapacitors can provide the best response to the changing needs of the electric motor.

In X.D. Xue's study, the operation of such a hybrid system is discussed, which is controlled by a device based solely on the SOC (state of charge) of the batteries and supercapacitors [13]. Our system's controller considers both the SOC and the current of the electric motor, meaning the current operating state. This makes the system more modern and adaptable to the demands of today's electric vehicles.

The implementation of the hybrid energy supply system is based on simulations in the Matlab/Simulink environment [5,14], as illustrated in Figure 18. The system includes a pack of three batteries providing 12 volts when fully charged, along with a supercapacitor, working together with a DC electric motor through a controller. Measurements showed that the motor works as expected, drawing 0.2 A under normal operation and 0.5 A at startup.

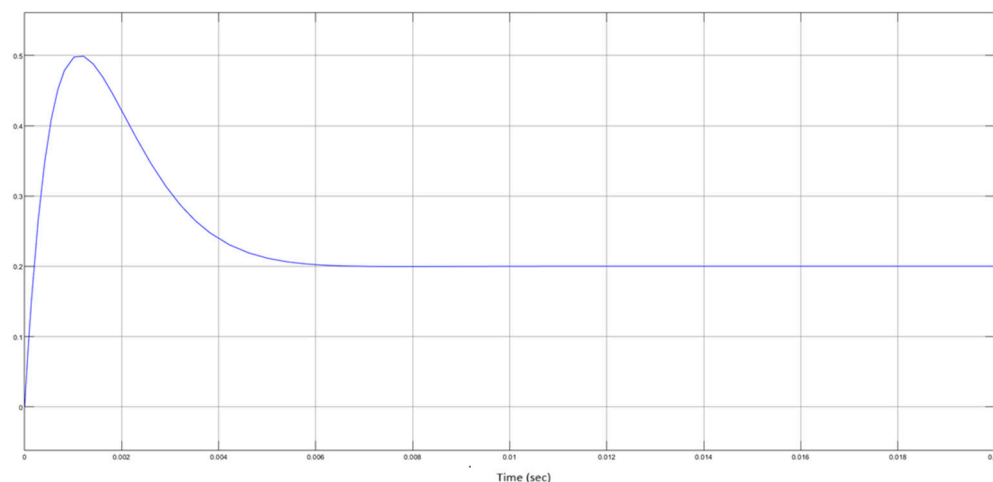


**Figure 18.** Increase of motor current at start-up.

The behavior of the battery voltage follows the typical discharge curve of Li-ion batteries, with a nearly vertical drop below 9 volts. This drop reflects how the batteries respond to loads, where the SOC decreases more quickly with an increasing load (Figure 19).

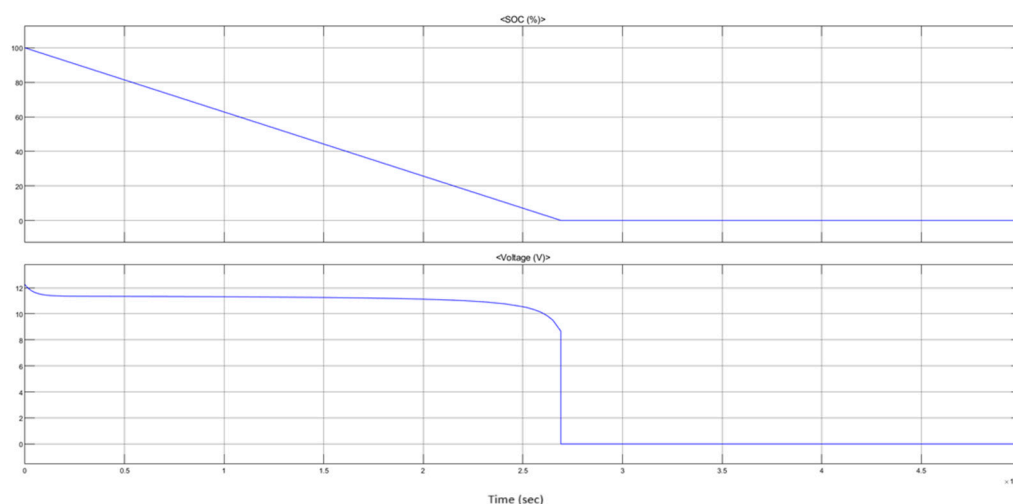


**Figure 19.** SOC and battery pack voltage for a constant current of 0.2 A.

In the supercapacitor system, a voltage converter keeps the output voltage at 12 volts. The simulations conducted for the supercapacitor are like those for the batteries. However, in the case of the supercapacitor, a minimal load is applied to the motor to ensure it operates at 0.33 A. Subsequently, a simulation is performed with an additional load (Figure 20).

The current, as in the case of the battery source, follows the behavior of the motor current; it shows a rise at start-up and then receives the value for the permanent state of the machine's operation. Its voltage and SOC decrease linearly, as expected, and reach zero in 12.5 min.

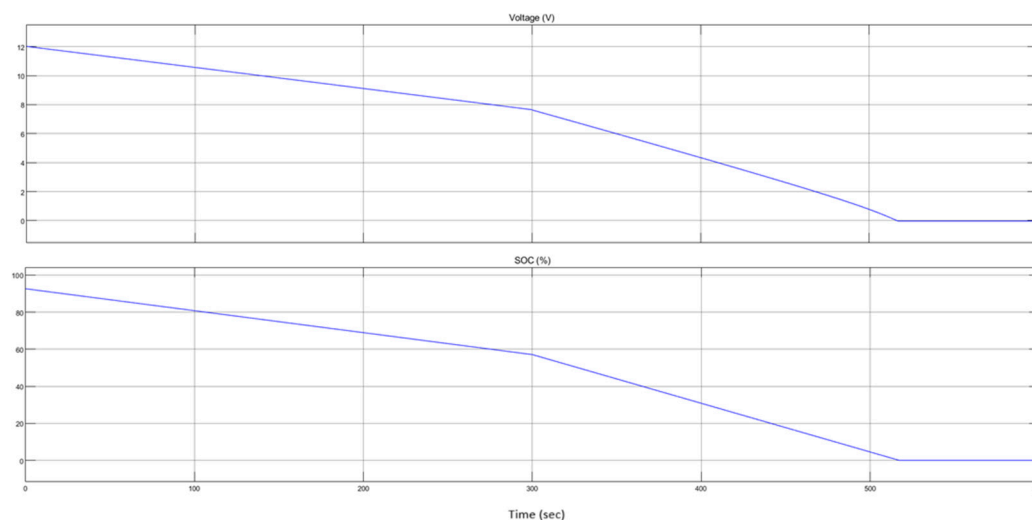


**Figure 20.** The supercapacitors' voltage and SOC with added motor load.

#### 4.1. Simulation of HESS Controller

The controller simulation is based on both the results of the simulations as well as the results of the laboratory experiments of each search of the hybrid system, and it is adapted to improve the operation of the power system. The results of the simulations and laboratory tests drew the following conclusions:

- In permanent operation, the motor draws 0.2 A, while in the starting tests, the current requested by the motor increases by 0.3–0.5 A;
- It was observed that when the voltage of the pack of three batteries was below 6 volts, the motor has difficulty turning and stops constantly. That is when the batteries can no longer power the motor. According to the simulations, when the battery voltage is equal to 2 volts, its SOC is 21%.

According to the above information of the laboratory and the simulations, the states of the controller are obtained as shown in Table 1 and Figure 21.

**Table 1.** States of HESS controller operation.

State	Motor Current (A)	Battery SOC (%)	Supercapacitors SOC (%)	Motor Power Source
A	<0.5	>80%	-	Battery Pack
B	>0.5	>80%	>0	SC Pack
C	<0.21	20% < SOC < 80%	-	Battery Pack
D	>0.21	20% < SOC < 80%	>0	SC Pack
E	-	<20%	>0	SC Pack
F	>0.5	-	>0	SC Pack
G	-	<20%	=0	Battery Pack
H	<0	-	-	SC Pack

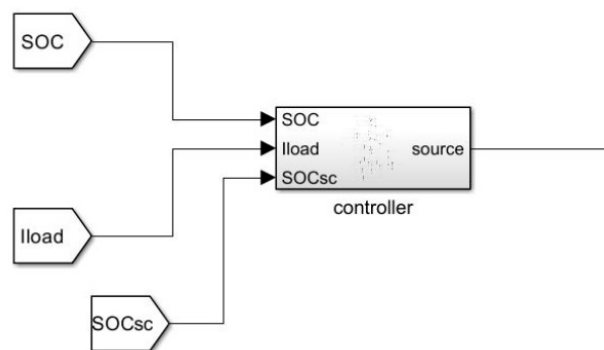


**Figure 21.** The HESS controller block in Simulink.

1. State A: If the SOC and voltage of the battery pack are above 80% (10.14 volts), and the motor current is below 0.5 A, the motor is powered by the batteries. This applies both in steady-state and during startup;
2. State B: If the SOC/voltage is above 80% (10.14 volts), and the motor current is above 0.5 A, the motor is powered by the supercapacitors. This condition applies during higher current demands, such as startup or when load is added to the motor shaft;
3. State C: When the SOC/voltage is between 80% (10.14 volts) and 20% (6 volts), and the current is below 0.21 A, the batteries are used. In this case, the batteries do not provide power during startup but only in steady-state operation;
4. State D: If the SOC/voltage is between 80% (10.14 volts) and 20% (6 volts), and the current is above 0.21 A, the supercapacitors are used;
5. State E: If the SOC/voltage is below 20% (6 volts) and the SOC of the supercapacitors is positive, the supercapacitors will be used regardless of current;
6. State F: If the motor current is above 0.5 A, the supercapacitors are used regardless of the SOC of the batteries;
7. State G: If the SOC/voltage is below 20% (6 volts), and the SOC of the supercapacitors is zero, the batteries will be used regardless of current;
8. State H: If the motor current is negative (indicating generator mode), the current will return to the supercapacitors [15].

For the supercapacitors to be used in all the above states, their SOC must be greater than zero.

The controller has three inputs:

- Motor Current: Measures the current required by the motor;
- Battery SOC: Represents the state of charge of the batteries;
- Supercapacitor SOC: Represents the state of charge of the supercapacitors.

The output of the controller is the voltage supplied to the motor, which can come from either the batteries or the supercapacitors.

The application of the controller is completed using logic gates and is divided into two sections:

1. The first section handles the states where the motor is powered by the batteries (States A, C, G);
2. The second section manages the states where the motor is powered by the supercapacitors (States B, D, E, F, H).

From these two sections, two control signals emerge: “bat” and “sc.” When the “bat” = 1, the motor is powered by the batteries; when “sc” = 1, the motor is powered by the supercapacitors. On the second part of the controller, a switch has also been added on the right side of the system, which decides which voltage will be input to the motor, that is,

what the basic output of the controller will be (Figures 22 and 23 represent the battery pack and supercapacitor control condition, respectively).

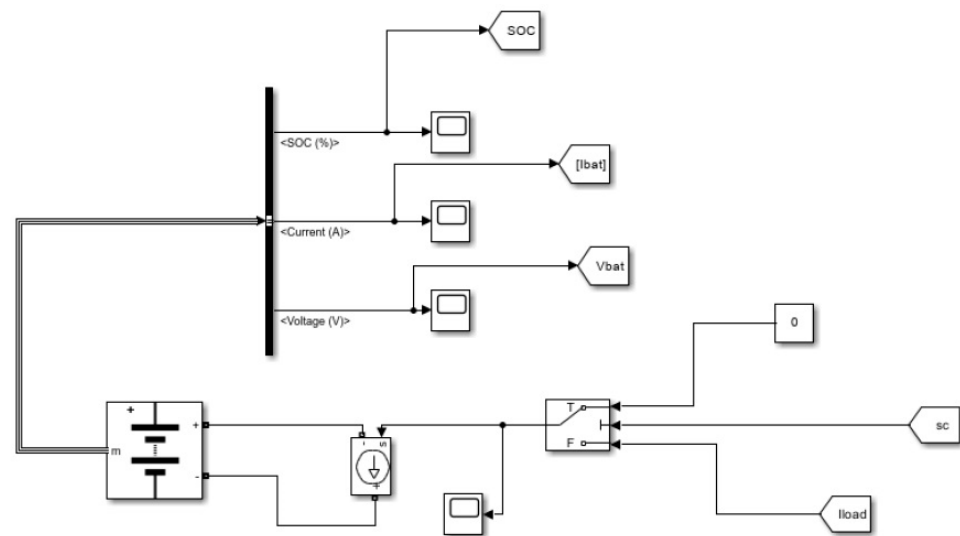


**Figure 22.** The battery pack with the control condition at its input.

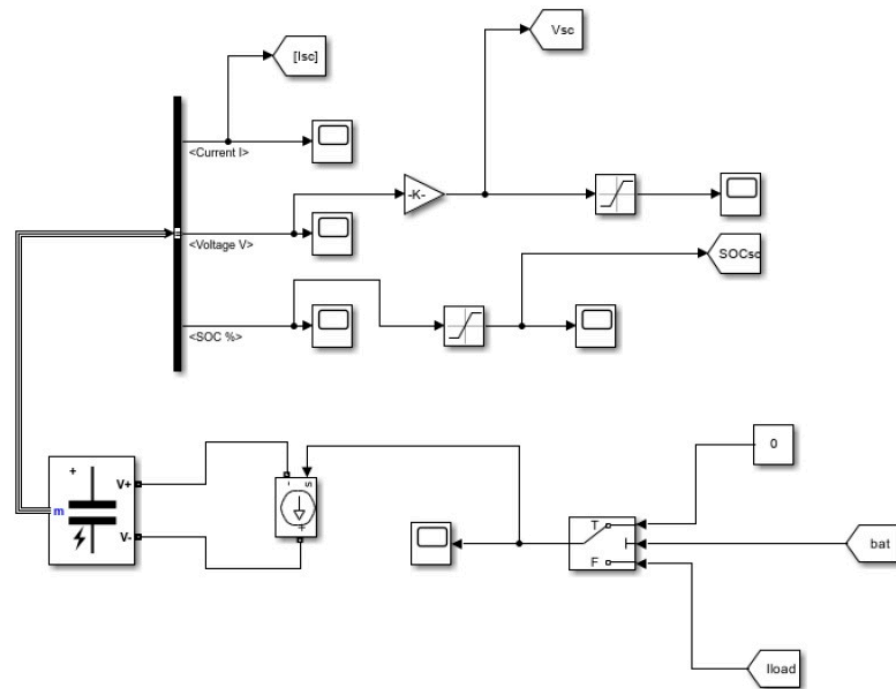


**Figure 23.** The supercapacitors with the control condition at its input.

## 4.2. Simulation Results

### 4.2.1. First Simulation (Operational States: A, B, C, D, F)

In this case, the motor current starts at approximately 0.9 A. Initially, the supercapacitors are activated until the current drops to 0.45 A, at which point the batteries are activated. When the state of charge (SOC) of the batteries reaches 80% and the current exceeds 0.21 A, the supercapacitors reactivate until they are depleted, after which the batteries continue to operate until the end of the simulation. This behavior is depicted in Figures 24 and 25 for the battery and supercapacitor, respectively.

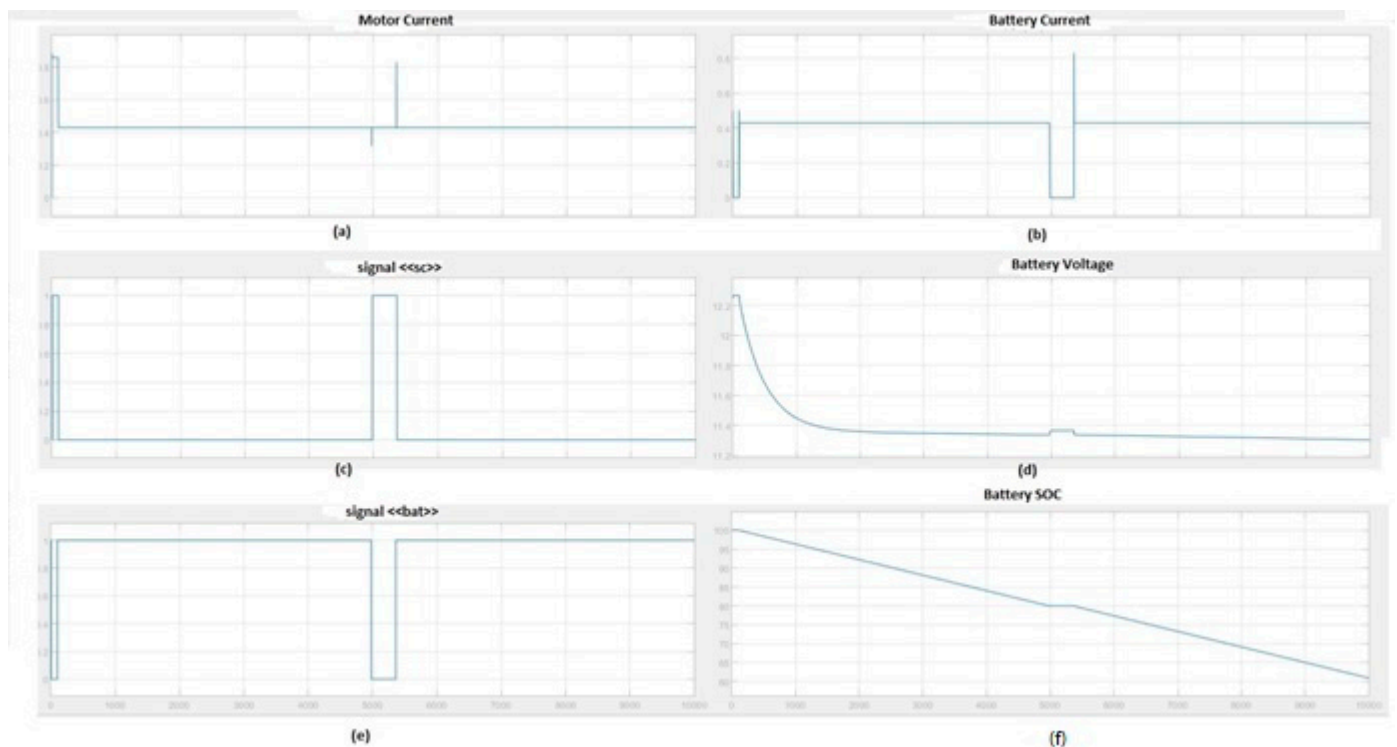


**Figure 24.** First battery simulation results: (a) Load current, (b) <<sc>> signal, (c) Signal <<bat>>, (d) Battery current, (e) Battery voltage, and (f) Battery SOC. X-axis represents time (s).

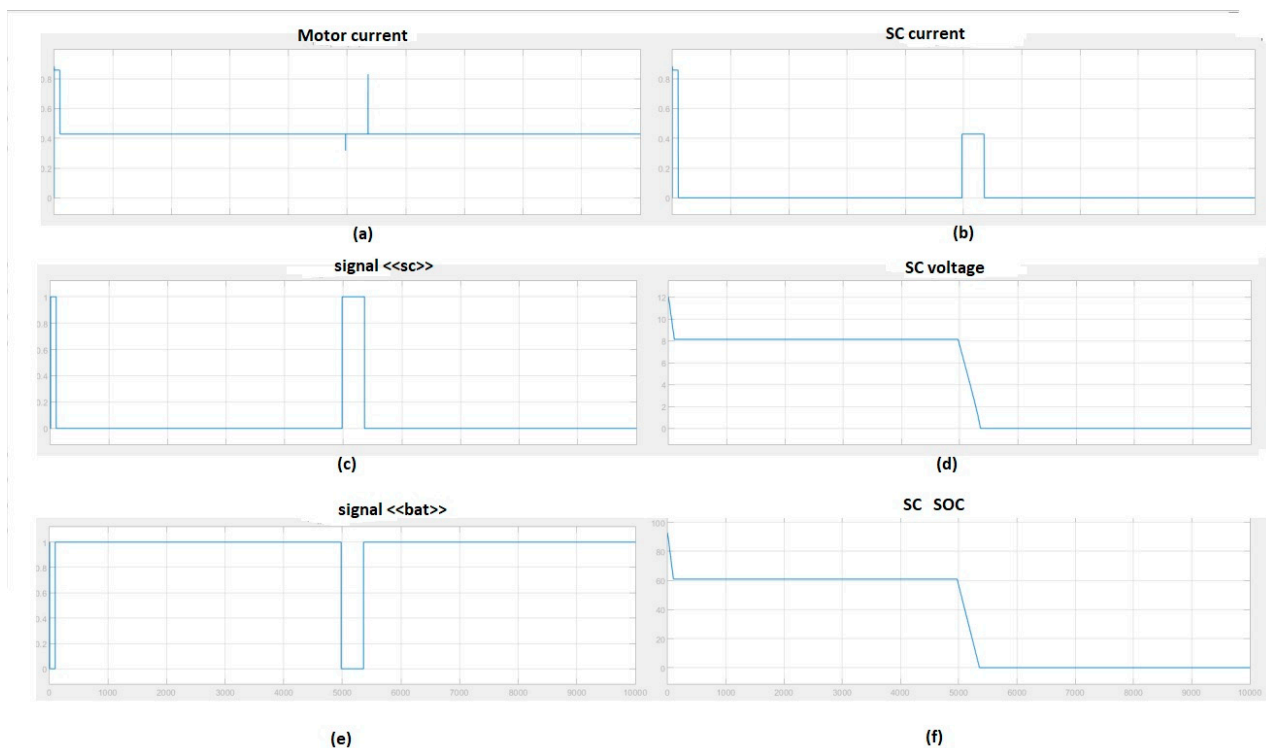


**Figure 25.** First supercapacitor simulation results: (a) Load current, (b) <<sc>> signal, (c) <<bat>> signal, (d) Supercapacitor current, (e) Supercapacitor voltage, and (f) Supercapacitor SOC. X-axis represents time (s).

#### 4.2.2. Second Simulation (Operational States: A, C, E, G)

The motor's current remains steady at 0.2 A throughout the simulation. The batteries discharge until the SOC reaches 20%, activating the supercapacitors. Supercapacitors

discharge quickly compared to batteries, which re-power the motor until they are fully discharged (Figures 26 and 27 represent the second battery and supercapacitor simulation results, respectively).

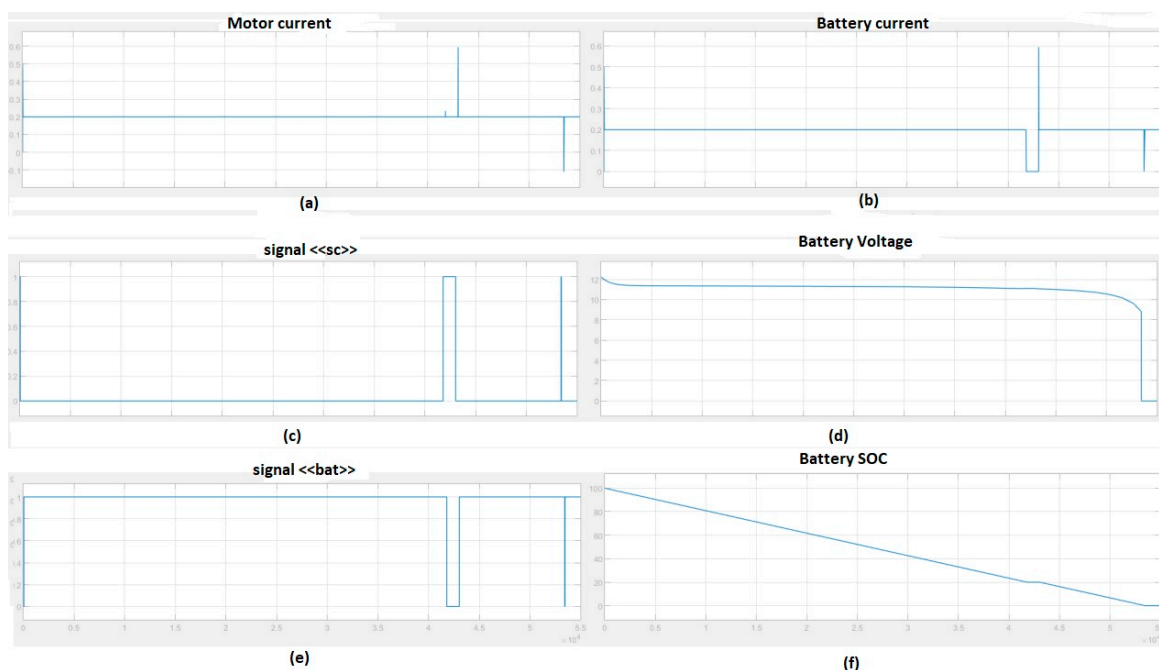


**Figure 26.** Second battery simulation results: (a) Load current, (b) <<sc>> signal, (c) Signal <<bat>>, (d) Battery current, (e) Battery voltage, and (f) Battery SOC.

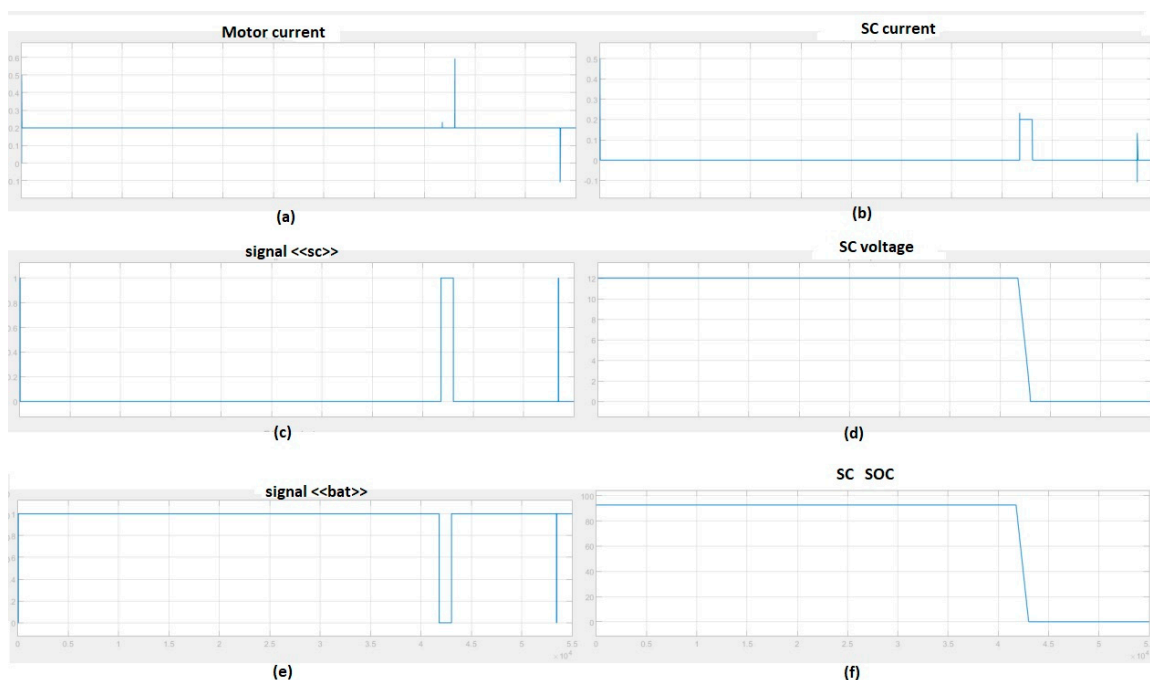


**Figure 27.** Second supercapacitor simulation results: (a) Load current, (b) <<sc>> signal, (c) <<bat>> signal, (d) Supercapacitor current, (e) Supercapacitor voltage, and (f) Supercapacitor SOC.

#### 4.2.3. Third Simulation (Operational States: F, H)

In this case, the batteries remain inactive. The current initially rises to approximately 0.9 A. Shortly thereafter, the motor switches to generator mode, charging the supercapacitors as the current turns negative. This simulation effectively demonstrates the concept



of regenerative braking. Figures 28 and 29 represent the third battery and supercapacitor simulation results, respectively.

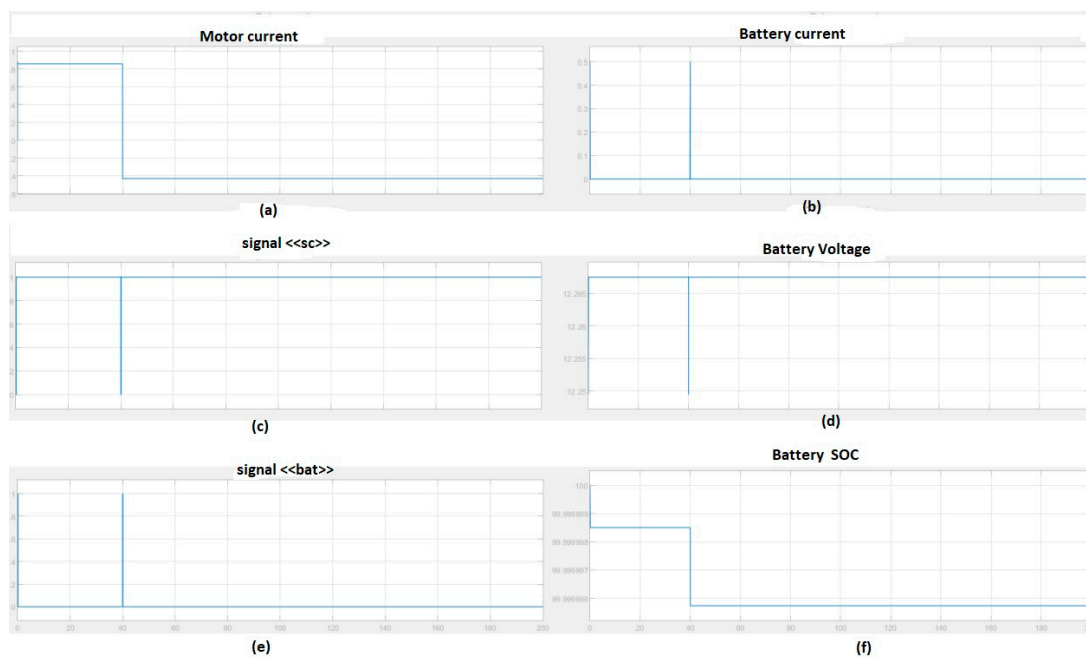


**Figure 28.** Third battery simulation results: (a) Load current, (b) <<sc>> signal, (c) Signal <<bat>>, (d) Battery current, (e) Battery voltage, and (f) Battery SOC.

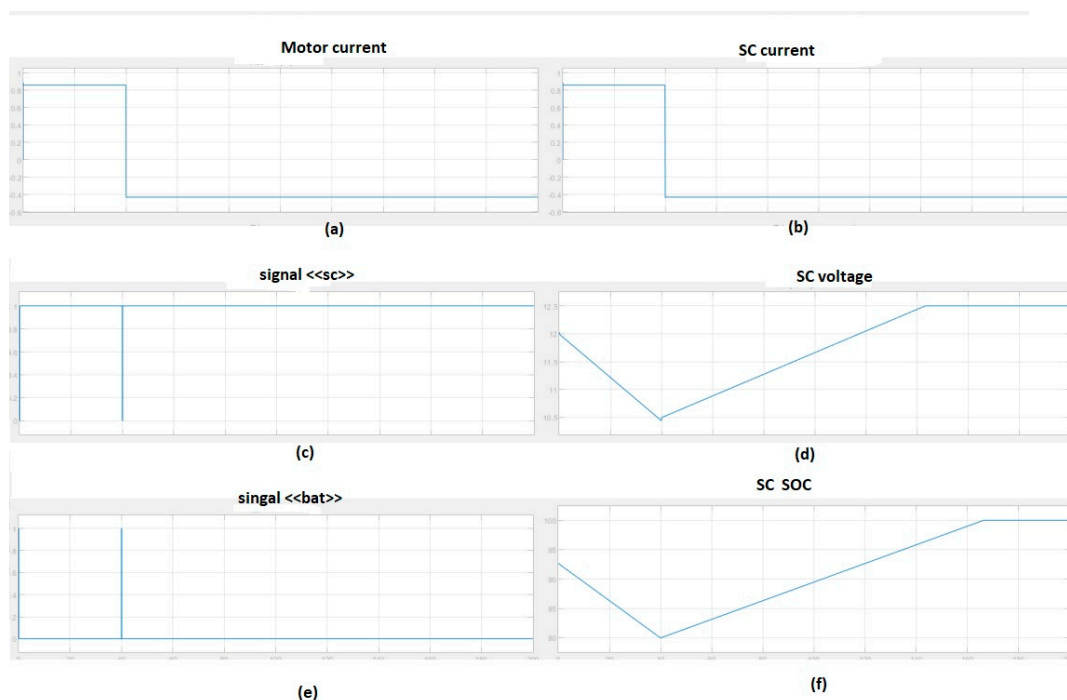


**Figure 29.** Third supercapacitor simulation results: (a) Load current, (b) <<sc>> signal, (c) <<bat>> signal, (d) Supercapacitor current, (e) Supercapacitor voltage, and (f) Supercapacitor SOC.

#### 4.3. Improvement in Battery Autonomy Performance with Use of HESS

In Table 1, the functional states of the hybrid system controller illustrated that the battery is protected during instances of high-power demand from the motor as well as when the charge level is low. These conditions correspond to functional state G of the controller, where the state of charge (SOC) of the batteries is below 20%. In these cases,

the supercapacitors will discharge fully before the batteries, which will only discharge completely under very specific circumstances.

The conclusion is that while the supercapacitors will routinely discharge fully and will recharge through the reverse flow of power during braking, the batteries will rarely reach low charge levels (SOC below 20%). This results in increased battery longevity, as seen with more frequent drops in SOC to critically low levels (Table 2).

**Table 2.** The capacity of the battery with the increase of its cycles compared as a main load source and a source in a hybrid system with supercapacitor.

Battery Cycles	Capacity (Ah), Battery as Main Source	Capacity (Ah), Battery as Part of Hybrid System
1	2.9133	2.9228
10	2.7891	2.8080
36	2.4167	2.4746
50	2.2151	2.2947
72	1.8972	2.0108
100	1.4946	1.6515
120	1.2080	1.3936
145	0.8478	1.0739

The simulations examined indicate that in the hybrid system, the battery capacity decreases at a slower rate. As shown in Table 2, after 50 charge–discharge cycles, the capacity of the battery in the simple system as the main power source is 2.2151 Ah, and while it is in the hybrid system, its capacity is 2.2947 Ah. After 100 cycles, the capacities have reduced to 1.4946 Ah and 1.6515 Ah, respectively. Finally, after 145 cycles, the capacities are 0.8478 Ah and 1.0739 Ah, respectively.

As previously mentioned in the preceding section, the autonomy of the system during the first cycle of the battery with a load current of 0.2 A is 14.5 h. The autonomy of the hybrid system during the 100th life cycle of the battery is 8.25 h, while in the simple power system, it is 7.5 h (Figure 30).

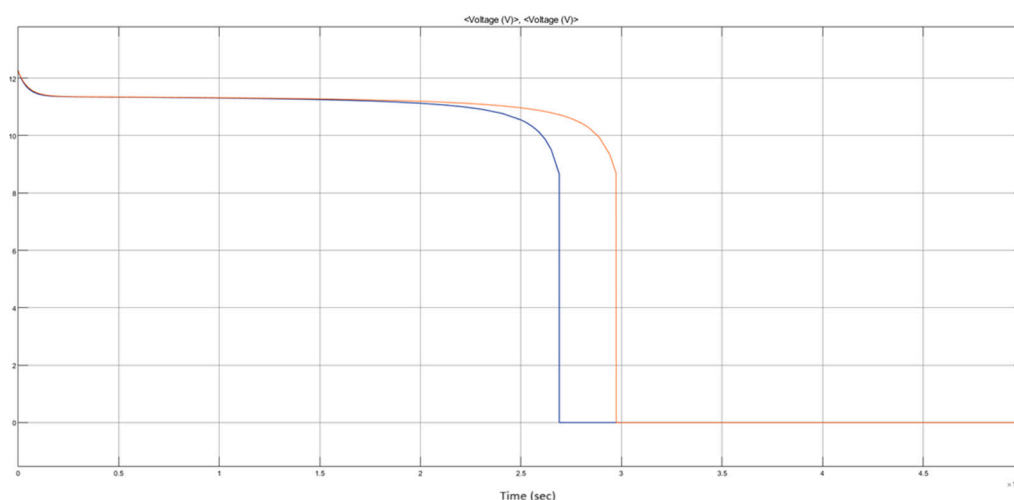


**Figure 30.** Battery discharging in its 100th cycle (The red curve corresponds to the hybrid system with a supercapacitor, and the blue curve corresponds to the simple system without a supercapacitor).

This leads us to conclude that by utilizing supercapacitors and developing the hybrid power system for the motor, we have improved the system's autonomy during the 100th charge-discharge cycle by 45 min.

Therefore, the improvement in battery performance with the incorporation of supercapacitors and the establishment of the hybrid power system is significant.

## 5. Conclusions

The simulations conducted for the battery cells demonstrated that discharge is directly related to the load current. Specifically, at a current of 0.2 A, the battery discharged fully in 14.5 h, with a slow initial decline in voltage followed by a sharp drop in the last 30 min of the process.

On the other hand, in the case of multiple charge-discharge battery cycles, it was observed that with a constant discharge current of 0.2 A and a charge current of 1 A, the battery capacity decreased from 2.9 Ah to 0.8 Ah after 145 cycles. This reduction renders the battery insufficient for powering the motor, highlighting the necessity of supercapacitors as a supplementary energy source.

The experimental results from testing a pack of three 2.9Ah batteries confirmed the predictions of the simulations, revealing a sharp decrease in voltage around the 24 h operating mark. Specifically, when the voltage at the battery pack terminals fell below 7 volts, the rotational speed of the motor significantly decreased, and when it dropped below 6 volts, the motor ceased operation. The 100 Farad supercapacitors, according to the simulations, fully charged in 45 min and discharged in 12 min, with discharge time significantly decreasing as the load current increased. This behavior is critical during startup and acceleration conditions for the motor, where the demand for high power is imperative.

The operation of the hybrid system relies on the controller, which determines which source will power the motor in each operational state. The controller not only monitors the status of the power sources but also collects data from the electric motor, adjusting its operation accordingly. As mentioned, the higher the motor's speed, the greater the current required. Specifically, during startup, the current is high. If the controller only considered the status of the energy sources, the system would be "blind" to such transient phenomena. Simulations demonstrated that the primary energy source for the motor is the batteries, with the supercapacitors primarily activating during transient operational events. This scenario enhances efficiency by allowing optimal use of the available resources, leveraging the advantages of both power sources. In conclusion, the hybrid system offers significant benefits in increasing the efficiency and autonomy of the power supply system while simultaneously reducing battery aging, thereby enhancing the sustainability of electric vehicles. Furthermore, future research could focus on adding battery thermal management technology as a parameter in the controller. This would help improve performance and further reduce battery aging, leading to better efficiency and sustainability of the hybrid system [16].

**Author Contributions:** Conceptualization, E.H. and M.K.; methodology, M.K.; validation, M.K., G.K., S.A., and E.H.; writing—original draft preparation, M.K. and G.K.; writing—review and editing, E.H., G.K., and M.K.; visualization, E.H. and M.K.; supervision, E.H. All authors have read and agreed to the published version of the manuscript.

**Funding:** This research received no external funding.

**Data Availability Statement:** The original contributions presented in this study are included in the article. Further inquiries can be directed to the corresponding author.

**Acknowledgments:** Acknowledgments are due to Emmanouela Mangiorou, Sensors Lab, School of Electrical Engineering, National TU of Athens. His collaboration was crucial for the successful completion of this study, and his assistance was essential for conducting the experiments.

**Conflicts of Interest:** The authors declare no conflicts of interest.

## References

1. Edge, J.S.; O’Kane, S.; Prosser, R.; Kirkaldy, N.D.; Patel, A.N.; Hales, A.; Ghosh, A.; Ai, W.; Chen, J.; Yang, J.; et al. Lithium Ion Battery Degradation: What You Need to Know. *Phys. Chem. Chem. Phys.* **2021**, *23*, 8200–8221. [CrossRef]
2. Thomas, A. *Using Supercapacitors in Electric Vehicles*; Technical Paper; KYOCERA AVX Components Corporation: Fountain Inn, SC, USA, 2022. Available online: <https://www.kyocera-avx.com/news/benefits-to-using-supercapacitors-in-electric-vehicles/> (accessed on 17 June 2024).
3. Lin, K. *A Control Strategy for Capacity Allocation of Hybrid Energy Storage System Based on Hierarchical Processing of Demand Power*; University of Chinese Academy of Sciences, Yanqihu Campus: Beijing, China, 2020. [CrossRef]
4. Yaseen, M.; Khan Khattak, M.A.; Humayun, M.; Usman, M.; Shah, S.S.; Bibi, S.; Syed Ul Hasnain, B.; Ahmad, S.M.; Khan, A.; Shah, N.; et al. A Review of Supercapacitors: Materials Design, Modification, and Applications. *Energies* **2021**, *14*, 7779. [CrossRef]
5. MathWorks. Getting Started with Simulink. Available online: [https://www.mathworks.com/help/simulink/getting-started-with-simulink.html?s\\_tid=CRUX\\_topnav](https://www.mathworks.com/help/simulink/getting-started-with-simulink.html?s_tid=CRUX_topnav) (accessed on 20 June 2024).
6. Lahbib, I.; Lahyani, A.; Sari, A.; Venet, P. Performance Analysis of a Lead-Acid Battery/Supercapacitors Hybrid and a Battery Stand-Alone Under Pulsed Loads. In Proceedings of the 2014 First International Conference on Green Energy (ICGE 2014), Sfax, Tunisia, 25–27 March 2014. Available online: <https://ieeexplore.ieee.org/document/6835434> (accessed on 8 July 2024).
7. Chipade, A.D.; Bhagat, V. Design and Analysis Hybrid Combination of Battery and Supercapacitor Using Orcad/Pspice. *Int. J. Res. Publ. Eng. Technol. (IJRPET)* **2017**, *3*, 64.
8. Analog Devices. LTspice Simulator. Available online: <https://www.analog.com/en/resources/design-tools-and-calculators/ltspice-simulator.html> (accessed on 20 June 2024).
9. Helseth, L. Modelling Supercapacitors Using a Dynamic Equivalent Circuit with a Distribution of Relaxation Times. *J. Energy Storage* **2019**, *25*, 100912. [CrossRef]
10. MIT Electric Vehicle Team. *A Guide to Understanding Battery Specifications*; MIT Electric Vehicle Team: Cambridge, MA, USA, 2008.
11. Ren, G. Introduction of SOC Estimation Method. *IOP Conf. Ser. Earth Environ. Sci.* **2021**, *687*, 012083. Available online: <https://iopscience.iop.org/article/10.1088/1755-1315/687/1/012083> (accessed on 11 May 2024). [CrossRef]
12. Cultura, A.B.; Salameh, Z.M. Modeling, Evaluation and Simulation of a Supercapacitor Module for Energy Storage Application. In Proceedings of the International Conference on Computer Information Systems and Industrial Applications (CISIA 2015), Bangkok, Thailand, 28–29 June 2015. [CrossRef]
13. Xue, X.D.; Raghu Raman, S.; Fong, Y.C.; Cheng, K.K. *Loss Analysis of Hybrid Battery-Supercapacitor Energy Storage System in EVs*; Proceedings Article; Power Electronics Research Centre, Department of Electrical Engineering, The Hong Kong Polytechnic University: Hong Kong, China, 2017. Available online: <https://ieeexplore.ieee.org/document/8277767> (accessed on 25 June 2024).
14. Ergin Şahin, M.; Blaabjerg, F. A Hybrid PV-Battery/Supercapacitor System and a Basic Active Power Control Proposal in MATLAB/Simulink. *Electronics* **2020**, *9*, 129. [CrossRef]
15. Lamprea de Jesus, F.R. *Design of a Supercapacitor/Battery Hybrid Energy Storage System for the TLMoto Prototype*; Técnico Lisboa: Lisbon, Portugal, 2019.
16. Jia, C.; Zhou, J.; He, H.; Li, J.; Wei, Z.; Li, K.; Shi, M. A novel energy management strategy for hybrid electric bus with fuel cell health and battery thermal- and health-constrained awareness. *Energy* **2023**, *271*, 127105. [CrossRef]

**Disclaimer/Publisher’s Note:** The statements, opinions and data contained in all publications are solely those of the individual author(s) and contributor(s) and not of MDPI and/or the editor(s). MDPI and/or the editor(s) disclaim responsibility for any injury to people or property resulting from any ideas, methods, instructions or products referred to in the content.